Title
Evaluating the Reproducibility of Mouse Anatomy under Rotation in a Custom Immobilization Device for Conformal FLASH Radiotherapy

Journal
Radiation Research, 194(6)

ISSN
0033-7587

Authors
Ko, Ryan B
Soto, Luis A
von Eyben, Rie
et al.

Publication Date
2020-12-01

DOI
10.1667/rade-20-00095

HHS Public Access

Author manuscript

Radiat Res. Author manuscript; available in PMC 2021 February 03.

Published in final edited form as:

Radiat Res. 2020 December 01; 194(6): 600–606. doi:10.1667/RADE-20-00095.

Evaluating the Reproducibility of Mouse Anatomy under Rotation in a Custom Immobilization Device for Conformal FLASH Radiotherapy

Ryan B. Ko[a], **Luis A. Soto**[a], **Rie von Eyben**[a], **Stavros Melemenidis**[a], **Erinn B. Rankin**[a,b,c], **Peter G. Maxim**[d,1], **Edward E. Graves**[a,c,1], **Billy W. Loo Jr.**[a,c,1]

[a]Department of Radiation Oncology, Stanford University School of Medicine, Stanford, California;

[b]Department of Obstetrics and Gynecology, Stanford University School of Medicine, Stanford, California;

[c]Stanford Cancer Institute, Stanford University School of Medicine, Stanford, California;

[d]Department of Radiation Oncology, Indiana University School of Medicine, Indianapolis, Indiana

Abstract

The observation of an enhanced therapeutic index for FLASH radiotherapy in mice has created interest in practical laboratory-based FLASH irradiators. To date, systems capable of 3D conformal FLASH irradiation in mice have been lacking. We are developing such a system, incorporating a high-current linear accelerator to produce a collimated X-ray beam in a stationary beamline design, rotating the mouse about a longitudinal axis to achieve conformal irradiation from multiple beam directions. The purpose of this work was to evaluate the reproducibility of mouse anatomy under rotation at speeds compatible with conformal FLASH delivery. Three short-hair mice and two hairless mice were immobilized under anesthesia in body weight-specific contoured plastic molds, and subjected to three rotational (up to 3 revolutions/s) and two non-rotational movement interventions. MicroCT images were acquired before and after each intervention. The displacements of 11 anatomic landmarks were measured on the image pairs. The displacement of the anatomical landmarks with any of the interventions was 0.5 mm or less for 92.4% of measurements, with a single measurement out of 275 (11 landmarks × 5 interventions × 5 mice) reaching 1 mm. There was no significant difference in the displacements associated with rotation compared to those associated with moving the immobilized mouse in and out of a scanner or with leaving the mouse in place for 5 min with no motion. There were no significant differences in displacements between mice with or without hair, although the analysis is limited by small numbers, or between different anatomic landmarks. These results show that anatomic reproducibility under rotation speed corresponding to FLASH irradiation times appears to be compatible with conformal/stereotactic irradiation in mice.

[1]Address for correspondence: Department of Radiation Oncology and Stanford Cancer Institute, Stanford University School of Medicine, 875 Blake Wilbur Drive, Stanford, CA 94305; bwloo@stanford.edu and egraves@stanford.edu; and Department of Radiation Oncology, Indiana University School of Medicine; pmaxim@iu.edu.

INTRODUCTION

Substantial interest in studying ultra-high dose-rate FLASH radiation therapy has recently been stimulated by a seminal study from Institut Curie (1), demonstrating an increased therapeutic index for FLASH (delivered at >40 Gy/s average dose rate) compared to conventional-dose-rate irradiation in mouse tumor models. Irradiation platforms used for preclinical FLASH research have included 4–20 MeV electron beams (1–5), 102 keV synchrotron X rays (6) and 138–230 MeV proton beams (7–9).

To translate these interesting preclinical findings to patient care, it is important to evaluate clinically relevant treatment conditions in the preclinical setting. Modern clinical radiation therapy is performed with conformal shaping of radiation doses in space, under image guidance, to cover the tumor target comprehensively while minimizing dose spill to surrounding normal organs. However, because of technical considerations, all FLASH research in mice to date has been constrained to irradiation of large body sections (e.g., head, thorax, abdomen) or the whole body rather than conforming to tumor targets in specific locations. Conformal irradiation requires sufficiently sharp collimation of the beam to the dimensions of targets in mice (e.g., as small as approximately 3 mm), and convergence of multiple beams from multiple directions around the subject. While X rays can be collimated with sufficiently sharp penumbra, conventional clinical energy electron and proton beams are not amenable to forming such narrow beams. Furthermore, to achieve overall dose rates for multi-beam conformal treatments within the FLASH dose-rate regimen, all the beams from different directions would have to be delivered within a fraction of a second. To date, such a preclinical system with the capability of pluridirectional delivery of FLASH radiation has not been developed.

To address this need, we are currently developing a laboratory-based image-guided FLASH experimental X-ray small-animal conformal therapy (FLASH-EXACT) system based on a novel linear accelerator design to produce much higher electron beam current (compared to conventional clinical systems) for conversion to X rays through bremsstrahlung (10). The conceptual schematic for this system is shown in Fig. 1. A commercial modulator/klystron supplies radiofrequency power to a compact next-generation 10 MeV electron linear accelerator (linac) with an average beam current of 1.5 mA, which produces a 10 MV collimated X-ray beam with a dose rate exceeding 50 Gy/s at 20–25 cm source to subject distance. This would correspond, for example, to a 20 Gy dose delivered in 0.4 s, which if distributed in a 360-degree arc, would correspond to 2.5 revolutions per second (Hertz; Hz) rotational speed around the isocenter. Because rotating the entire treatment system around a mouse at that speed is practically prohibitive, we propose a fixed beam delivery system in which the subject rotates relative to the beam. CT image guidance would be achieved by incorporating a kV X-ray source and detector that acquires images as the subject rotates on the same axis as the treatment isocenter.

In this study, we evaluated the reproducibility of mouse anatomy under rotation at rates up to 3 Hz in a custom immobilization device to assess the feasibility of this concept for conformal stereotactic FLASH irradiation. We sought to determine whether factors such as mouse body hair, anatomic location, and rotational and non-rotational positioning

interventions induce anatomic shifts sufficient to effect conformal/stereotactic irradiation accuracy.

MATERIALS AND METHODS

All procedures for use of animals and their care were approved by the Institutional Animal Care and Use Committee of Stanford University in accordance with institutional and NIH guidelines.

Mice, Positioning Interventions and In Vivo Imaging

To investigate the factor of hair in anatomic reproducibility under rotation, we studied two mouse strains, C57BL/6 (n = 3) and NU/NU nude (n = 2) mice (strain codes 027 and 088; Charles River Laboratories, Wilmington, MA), with and without hair, respectively. Mice were immobilized within body conforming animal molds (BCAMs; InVivo Analytics, New York, NY), which are body weight-specific plastic shells that conform to the mouse body shape, as shown in Fig. 2A. Mice were anesthetized with a 10:1 cocktail of ketamine (100 mg/kg) and xylazine (10 mg/kg) administered intraperitoneally, and the mice were checked frequently for respiratory status. BCAMs have been previously characterized with respect to reproducibility of mouse organ positioning (11). The BCAMs are available in a range of sizes corresponding to 2 g increments of mouse body weight, and the appropriate one was chosen according to the weight of each mouse.

Three different types of positioning interventions were tested: 1. moving the mouse, immobilized in the BCAM, out of the microCT scanner to a tabletop then back again without rotation; 2. placing the BCAM-immobilized mouse inside a polyvinyl chloride (PVC) pipe and rolling it down a halfpipe ramp (Tony Hawk Circuit Boards Halfpipe Ramp; Innovation First Labs Inc., Greenville, TX) with a starting height such that the maximum rotational speed was up to 3 Hz; and 3. no motion, leaving the BCAM-immobilized mouse in place within the microCT scanner for 5 min. For the rotation intervention shown in Fig. 2B, rotational speed was determined by marking the PVC pipe with tape and recording video at 30 frames/s during the halfpipe ramp roll using the camera of an iPhone 7 (Apple Inc., Cupertino, CA).

MicroCT images were acquired before and after the interventions, as shown in Fig. 2C, using the CT scanner of the X-RAD SmART system (Precision X-ray Inc., North Branford, CT). The region of interest included the full body of the mouse encapsulated in a BCAM with approximately one half of the tail in view. For the microCT imaging protocol, the following parameters were used: tube voltage 80 kVp, tube current 1 mA, helical pitch 200 μm, capture speed 15 fps and section thickness 0.4 mm. Image reconstructions were performed at 0.4 mm section thickness. Acquired images were contiguous.

The sequence of interventions and images is shown in Fig. 2D. The halfpipe ramp rolls were repeated three times for each mouse.

Landmark Displacement Analysis

All microCT images were analyzed using MIM Maestro version 6.6.5 (Cleveland, OH). Eleven landmark point contours were manually segmented for each scan (by RBK, verified by BWL) at reproducibly identifiable locations spanning cranial to caudal regions including the head (tip of the left incisor, opisthocranion, right anterolateral tip of the interparietal bone; Fig. 3A), thorax (carina, T8 and L1 vertebrae; Fig. 3B), abdomen (right renal hilum, left renal hilum, L5 vertebra; Fig. 3C), and pelvis (left SI joint, pubic symphysis; Fig. 3D).

Scans before and after each intervention were rigidly registered in a pairwise fashion, using the BCAM as the reference. Displacements between each pair of scans were calculated for all 11 landmarks, producing a total of 275 measurements (11 landmarks × 5 interventions × 5 mice). Differences between measured parameters were analyzed using a mixed-effects model to account for within-mouse correlations. Pairwise comparisons were made in a post hoc analysis with a Tukey adjustment for multiple comparisons.

RESULTS

Mouse Rotation

The five mice weighed between 20.4 and 26.9 g. All image acquisitions were successful for all subjects. The ramp rolls were reproducible with an average maximum rotation speed of 2.6 Hz. Based on the shape of the ramp, the mice underwent several revolutions in opposite directions as they rolled up and down the sides of the halfpipe until they gradually came to rest (Fig. 2B). The mean total number of revolutions was 10.0 ± 2.9 per mouse for an average duration of 7.2 ± 2.0 s. Halfpipe ramp roll data are provided in Table 1.

Anatomic Displacement

The mean displacement for all landmarks in all subjects was 0.21 mm ± 0.19 (standard deviation) with a range of 0.01 mm to 1.00 mm. The maximum displacement of 1.00 mm occurred at the tip of the left incisor in a nude mouse with the first ramp roll. Figure 4 shows a representative displacement analysis for one of the mice in which CT intensity differences are superimposed on rigidly registered microCT image pairs from before and after each intervention.

Figure 5 shows the distribution of all anatomic landmark displacements, where 92.4% of all displacements were 0.5 mm or less in magnitude across all interventions. For both rotational and non-rotational interventions (moving in and out of scanner or leaving in place), over 90% of displacements (93.3% for rotational and 90.9% for non-rotational) were 0.5 mm or less.

Figure 6 shows the adjusted mean values based on the mixed-effects model for anatomic displacements by intervention and per landmark for C57BL/6 and NU/NU mice. The differences between interventions were associated with a P value of 0.0428, and the largest average displacement of 0.26 mm was associated with the first roll. However, a displacement of 0.26 mm would not affect the accuracy of stereotactic treatment of targets in the ~3 mm size range. There was a trend toward interaction between mouse hair type and anatomical

landmark displacement (P 0.0588). The median displacement for all landmarks in the C57BL/6 and NU/NU mice were 0.13 and 0.15 mm, respectively. The nude mice had a slightly greater displacement across all anatomical landmarks with the largest differences at the left incisor and the pubic symphysis. For these two landmarks, the nude mice had a displacement that was 0.17 mm and 0.16 mm larger, respectively, than the displacement of the C57BL/6 mice. Again, these differences are too small to affect the accuracy of stereotactic irradiation. Furthermore, after a Tukey adjustment for multiple comparisons, all P values were >0.05.

DISCUSSION

In this study, we completed a series of translational and rotational movements in five mice and measured the anatomical displacement with microCT. These movements were intended to simulate that of a mouse rotation stage in a prototype conformal FLASH irradiator with a stationary single-beam line. We found that the displacement of multiple reference anatomical landmarks was 0.5 mm or less in over 90% of measurements, with a single measurement (out of 275) reaching 1 mm. There was no relevant difference in the displacements associated with rotation compared to those associated with moving the immobilized mouse in and out of a scanner or with leaving the mouse in place for 5 min with no motion. This suggests that stereotactic positioning accuracy under relatively rapid mouse rotation is achievable.

We evaluated rotation speeds compatible with conformal FLASH irradiation. At a rotation speed of 3 revolutions/s (Hz), a full rotation would be completed within 333 ms and a half rotation within 167 ms, sufficient to deliver 8–16 Gy conformally at a dose rate of 50 Gy/s, for example. As a point of reference, with an approximate width of 2 cm for a mouse, even with an eccentric axis of rotation in which the outer part of the mouse is at a radius of 1.5 cm from the axis, at 3 Hz the maximum centrifugal acceleration would only be approximately one half that of gravity.

Our study is similar in some respects to previously published work evaluating anatomic deformation under rotation of rabbits and human volunteers in the context of a proposed compact and economical fixed beamline clinical radiotherapy system with a geometry analogous to our FLASH-EXACT preclinical system (12, 13). Those studies evaluated much slower rotation speed in keeping with conventional-dose-rate delivery used clinically, and focused on gravity-induced deformation at different angular positions, finding relatively small (on the order of 5 mm) displacements compared to the size of the subjects. Our study was focused on anatomic stability under rapid rotation.

A number of mouse stereotactic positioning systems have been developed for preclinical irradiation (4, 5, 11). In this study we evaluated one designed for multi-modality small animal imaging, that has previously been shown to achieve reproducible mouse organ positioning and a snug fit within the rigid form-fitting shell with minimal air gap (11). This, combined with the much smaller size and mass of mice, likely contributes to the sub-millimeter displacements observed in this study compared to the rabbit and human studies.

We used short-hair and hairless mice to test the hypothesis that skin-to-plastic contact would provide greater stability. We did not observe a relevant difference between these two cohorts, with minimal displacements in both cases. This study is dependent on the ability of BCAMs to conform to and immobilize subjects effectively. Future work is needed to evaluate the suitability of body weight-specific BCAMs to immobilize mice of different strains as well as mice bearing subcutaneous tumors that may not be well matched by the BCAM shape.

The limitations of this study revolve around our available equipment and analytical approach. The sub-millimeter displacements we observed were near the resolution limit imposed by the 0.4 mm voxel size of our microCT scanner. We also chose mostly skeletal landmarks for displacement analysis owing to the soft tissue contrast limitations of CT. A future improvement could be the use of MRI instead of CT to improve the soft tissue contrast. Deformable image registration and deformation vector field analysis could provide a more comprehensive assessment of anatomic deformation owing to rotation. On the other hand, the ramp roll technique we used produced many more revolutions than would be applied by our proposed treatment system, suggesting that the displacements we observed might overestimate the displacements expected for a single revolution during FLASH irradiation.

CONCLUSION

This proof-of-concept study evaluates the reproducibility of mouse anatomy after repeated rotations at speeds compatible with practical implementation of a preclinical conformal FLASH radiotherapy system. We demonstrate that anatomic displacement was well below 1 mm. This indicates feasibility of volumetric image-guidance and treatment of rotated mice subjects with a stationary, single-beam, conformal FLASH irradiator.

ACKNOWLEDGMENTS

We thank InVivo Analytics, Inc. for providing samples of the body-conforming animal molds for evaluation. We also acknowledge Adam Neff and Krista Curry-Jones (MIM Software, Inc.) for technical assistance with image analysis. This research was supported by funds from the National Cancer Institute (NCI grant no. 1P01CA244091-01) and the Department of Radiation Oncology, Stanford University School of Medicine. We also gratefully acknowledge the generous support of philanthropic donors to the Department of Radiation Oncology. BWL, EEG and PGM have received research support from Varian Medical Systems. BWL and PGM are co-founders of TibaRay. BWL is a board member of TibaRay.

REFERENCES

1. Favaudon V, Caplier L, Monceau V, Pouzoulet F, Sayarath M, Fouillade C, et al. Ultrahigh dose-rate FLASH irradiation increases the differential response between normal and tumor tissue in mice. Sci Transl Med 2014; 6:245ra93.
2. Jaccard M, Duran MT, Petersson K, Germond JF, Liger P, Vozenin MC, et al. High dose-per-pulse electron beam dosimetry: Commissioning of the Oriatron eRT6 prototype linear accelerator for preclinical use. Med Phys 2018; 45:863–74. [PubMed: 29206287]
3. Lempart M, Blad B, Adrian G, Back S, Knoos T, Ceberg C, et al. Modifying a clinical linear accelerator for delivery of ultra-high dose rate irradiation. Radiother Oncol 2019; 139:40–5. [PubMed: 30755324]
4. Levy K, Natarajan S, Wang J, Chow S, Eggold J, Loo P, et al. FLASH irradiation enhances the therapeutic index of abdominal radiotherapy in mice. bioRxiv 2019:2019.12.12.873414.

5. Schuler E, Trovati S, King G, Lartey F, Rafat M, Villegas M, et al. Experimental platform for ultra-high dose rate FLASH irradiation of small animals using a clinical linear accelerator. Int J Radiat Oncol Biol Phys 2017; 97:195–203. [PubMed: 27816362]

6. Montay-Gruel P, Bouchet A, Jaccard M, Patin D, Serduc R, Aim W, et al. X-rays can trigger the FLASH effect: Ultra-high dose-rate synchrotron light source prevents normal brain injury after whole brain irradiation in mice. Radiother Oncol 2018; 129:582–8. [PubMed: 30177374]

7. Diffenderfer ES, Verginadis II, Kim MM, Shoniyozov K, Velalopoulou A, Goia D, et al. Design, implementation, and in vivo validation of a novel proton FLASH radiation therapy system. Int J Radiat Oncol Biol Phys 2020; 106:440–8. [PubMed: 31928642]

8. Kim MM, Irmen P, Shoniyozov K, Verginadis II, Cengel KA, Koumenis C, et al. Design and commissioning of an image-guided small animal radiation platform and quality assurance protocol for integrated proton and X-ray radiobiology research. Phys Med Biol 2019; 64:135013. [PubMed: 31075786]

9. Patriarca A, Fouillade C, Auger M, Martin F, Pouzoulet F, Nauraye C, et al. Experimental set-up for FLASH proton irradiation of small animals using a clinical system. Int J Radiat Oncol Biol Phys 2018; 102:619–26. [PubMed: 30017793]

10. Maxim PG, Tantawi SG, Loo BW Jr. PHASER: A platform for clinical translation of FLASH cancer radiotherapy. Radiother Oncol 2019; 139:28–33. [PubMed: 31178058]

11. Klose AD, Paragas N. Automated quantification of bioluminescence images. Nat Commun 2018; 9:4262. [PubMed: 30323260]

12. Whelan B, Liney GP, Dowling JA, Rai R, Holloway L, McGarvie L, et al. An MRI-compatible patient rotation system – design, construction, and first organ deformation results. Med Phys 2017; 44:581–8. [PubMed: 27992058]

13. Barber J, Shieh CC, Counter W, Sykes J, Bennett P, Ahern V, et al. A CBCT study of the gravity-induced movement in rotating rabbits. Phys Med Biol 2018; 63:105012. [PubMed: 29667933]

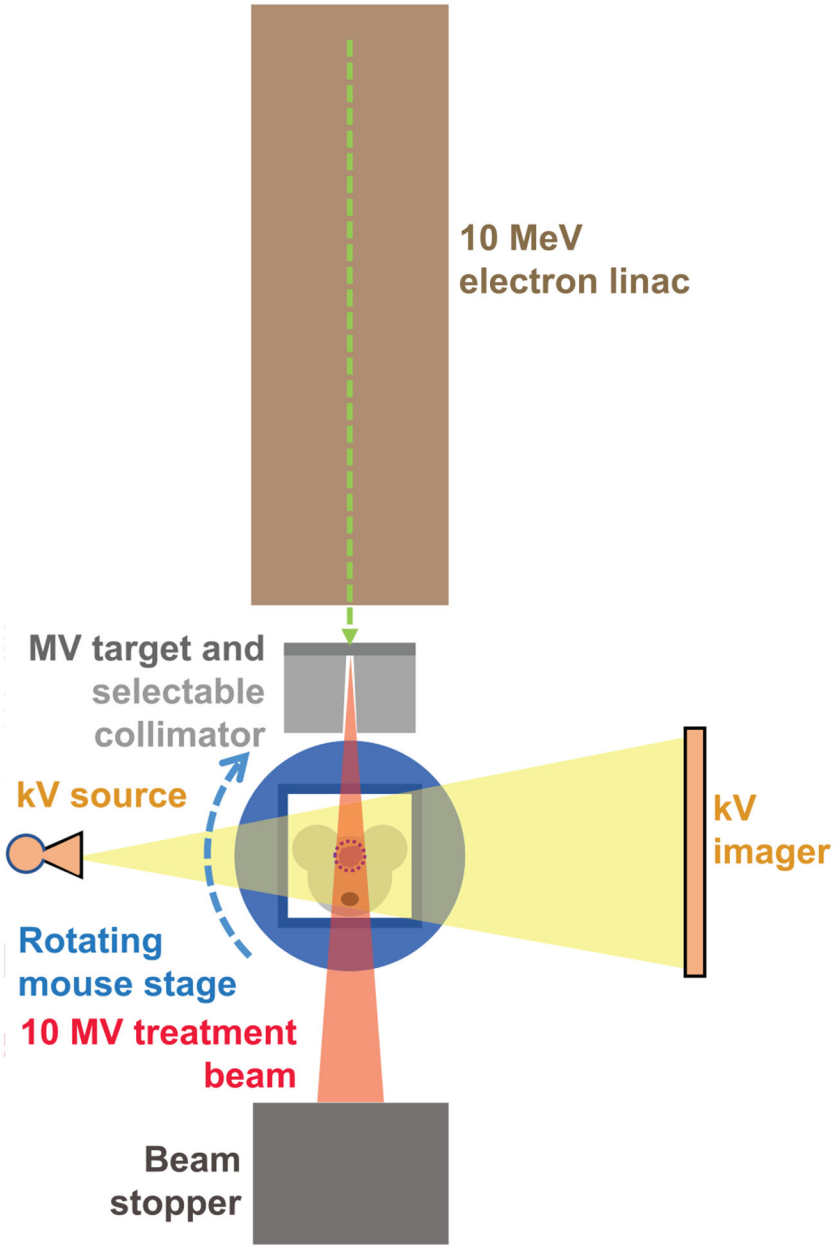

FIG. 1.

Conceptual schematic of the FLASH experimental X-ray small animal conformal therapy (FLASH-EXACT) system currently being developed. A next-generation compact electron linac produces a high current (1.5 mA average), 10 MeV beam that generates X rays through bremsstrahlung for FLASH dose rates exceeding 50 Gy/s at 20–25 cm from the X-ray source. The collimated X-ray beam is directed toward the mouse target at the isocenter. The mouse is immobilized securely within a body weight-specific conforming mold, and rotated relative to a kV X-ray source/detector combination for CT imaging, and the 10 MV X-ray treatment beam for conformal arc irradiation, both of which are stationary and share a common isocenter.

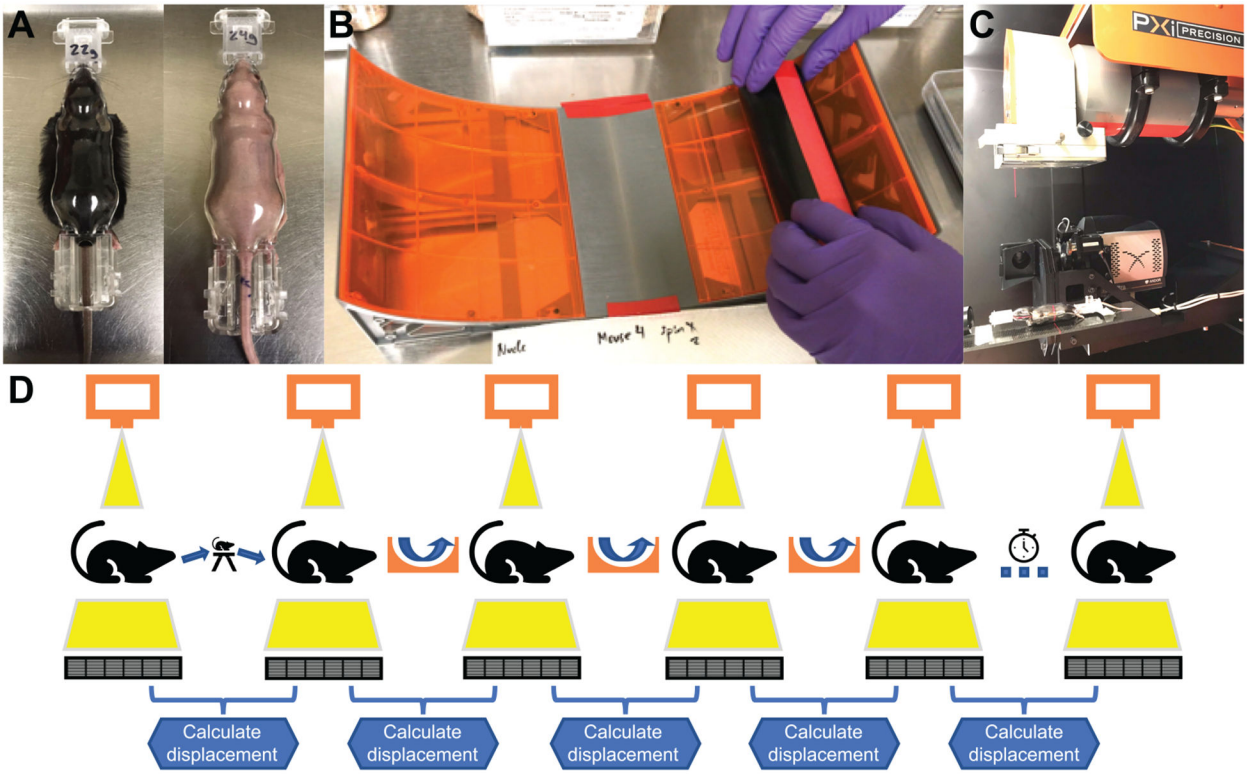

FIG. 2.

Panel A: A C57BL/6 mouse and NU/NU mouse were secured in body weight-specific body-conforming animal molds (BCAMs). Panel B: Mouse within a BCAM secured in PVC pipe is rolled down a halfpipe ramp at a maximum rotational speed of 3 revolutions/s. Panel C: Mouse imaged on microCT scanner. Panel D: Schematic of the experimental protocol. MicroCT images are taken before and after moving the BCAM-immobilized mouse out of the scanner and back without rotation, before and after each of three halfpipe ramp rolls, and before and after leaving the mouse in place for 5 min in the scanner without motion. Landmark displacement was calculated for 11 anatomic landmarks between microCT images before and after each intervention.

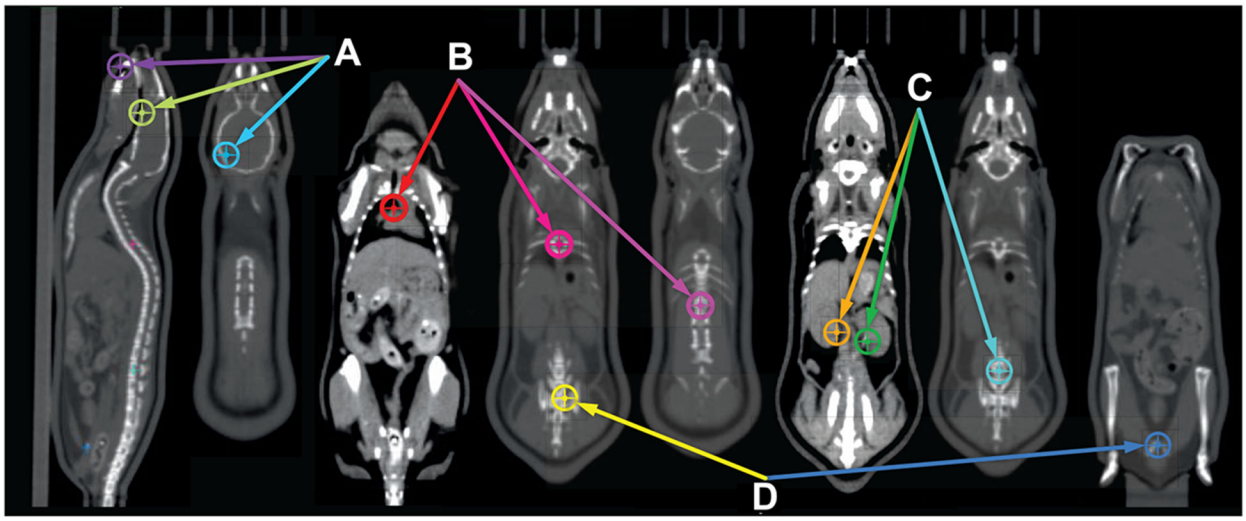

FIG. 3.

A consistent set of 11 anatomic landmarks was manually segmented on each microCT scan to calculate anatomic displacement before and after each intervention. Landmarks spanned cranial to caudal regions, as follows: (A) The head (tip of the left incisor, opisthocranion, right anterolateral tip of the interparietal bone); (B) The thorax (carina, T8 and L1 vertebrae); (C) The abdomen (right and left renal hila, L5 vertebra); and (D) The pelvis (left sacroiliac joint, pubic symphysis).

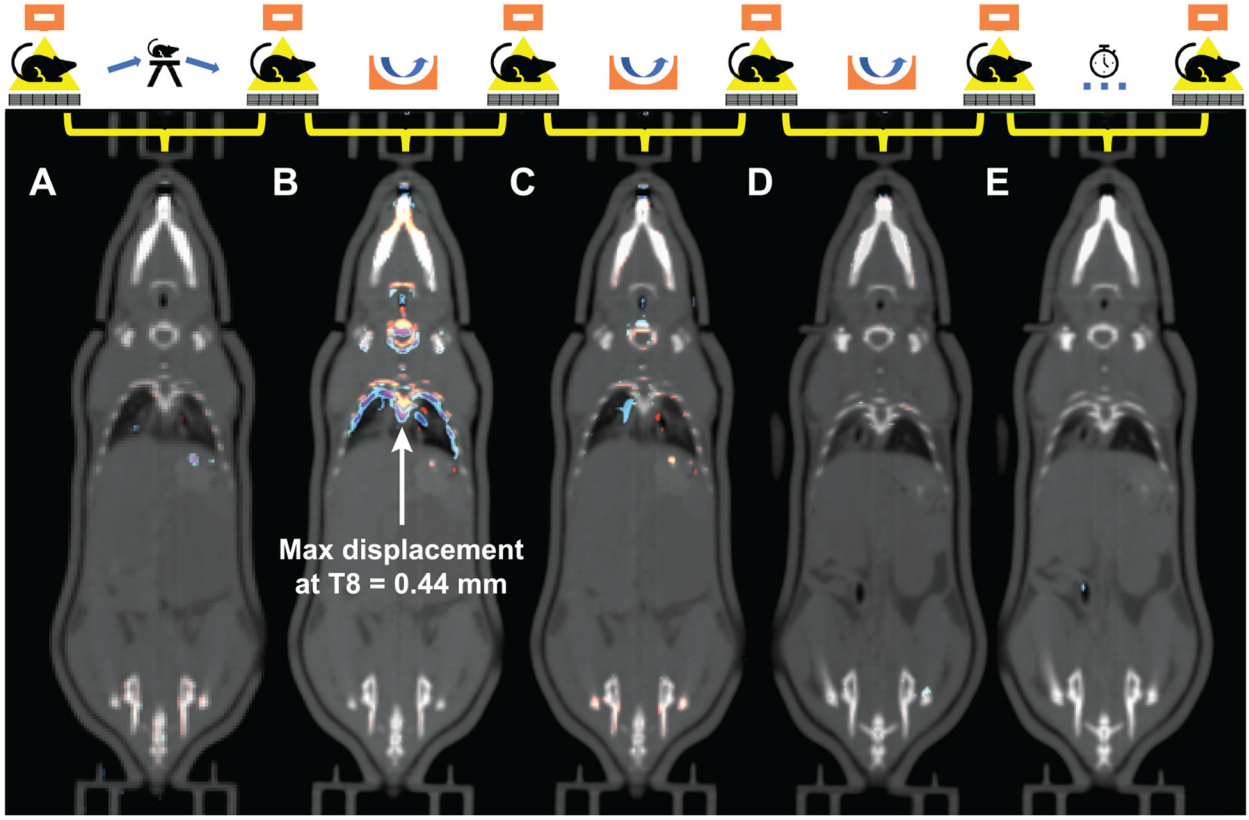

FIG. 4.

A representative analysis of anatomic displacements in one of the mice. Pairs of microCT images from before and after each intervention were rigidly registered using the immobilization mold as the reference. The interventions were: (A) Moving the BCAM-immobilized mouse out of the scanner and back without rotation; (B–D) Three halfpipe ramp rolls; and (E) Leaving the mouse in place for 5 min. The difference maps are superimposed on the images showing the normalized intensity differences from the initial (blue) to subsequent (red) scans. In this case, the largest displacement occurred with the first rotational intervention, but with the maximum displacement of any of the landmarks of only 0.44 mm at the T8 vertebra.

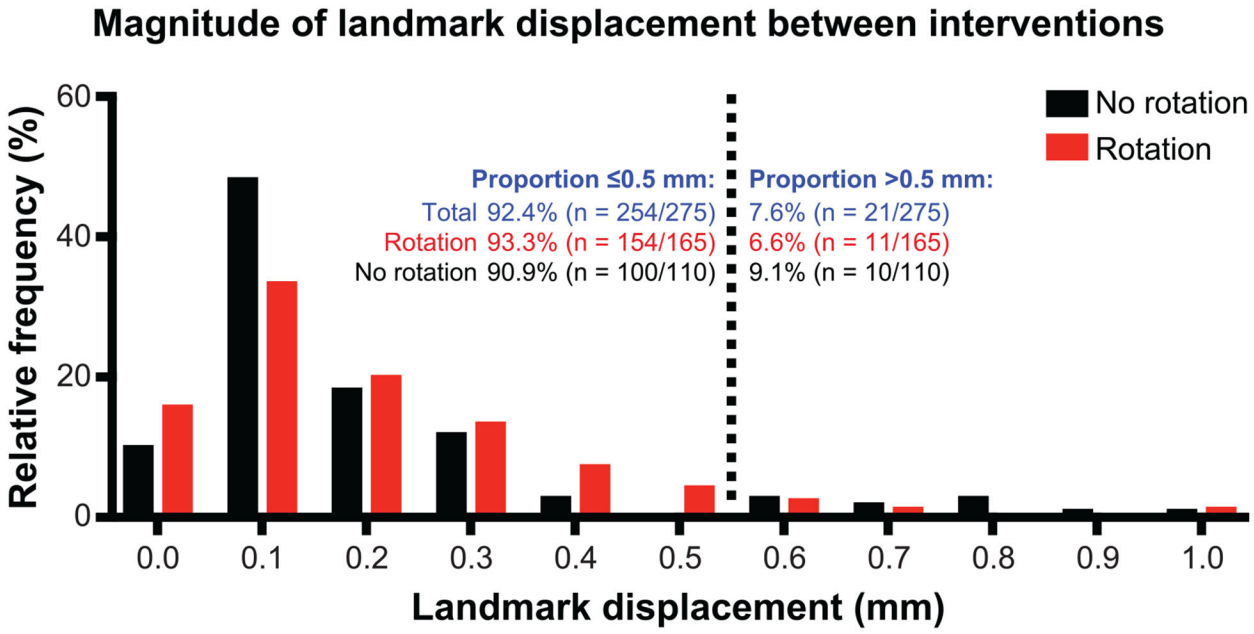

FIG. 5.

Frequency distribution (histogram) of all anatomic landmark displacements. Of all displacement measurements, 92.4% (254/275) were 0.5 mm or less. The maximum displacement of any landmark was 1.0 mm. For both rotational and non-rotational interventions (moving in and out of scanner or leaving in place), over 90% of displacements (93.3% for rotational and 90.9% for non-rotational) were 0.5 mm or less.

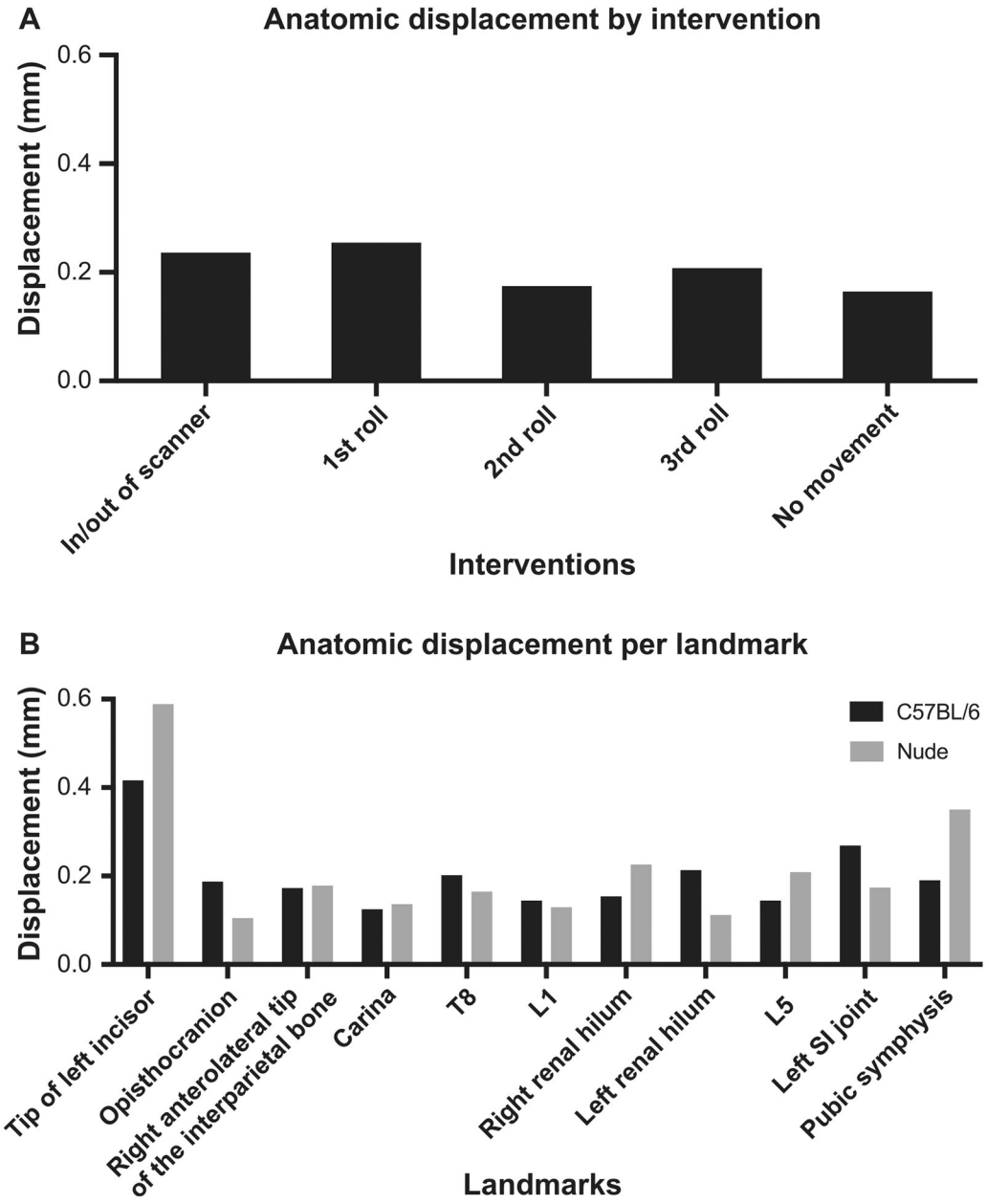

FIG. 6.

Panel A: Anatomic displacement by intervention for all mice. The largest displacements were associated with the first roll (mean 0.255 mm). Panel B: Anatomical displacement per landmark for C57BL/6 and nude mice. The anatomic landmark with the largest displacement was the tip of the left incisor. The nude mice had a slightly greater displacement across all anatomical landmarks with the largest differences at the left incisor and the pubic symphysis (0.17 mm and 0.16 mm larger, respectively, than the displacement of the C57BL/6 mice). All of these magnitudes are too small to affect the accuracy of stereotactic irradiation of targets ~3 mm in size, and none were statistically significant.

TABLE 1

Halfpipe Ramp Roll Data for All Mouse Subjects

Mouse	Intervention	CCW revolutions	CW revolutions	Total revolutions	Maximum velocity (rev/s)	Total duration (s)
C57BL/6 no. 1 (21.9 g)	1st roll	3.25	5.25	8.5	3.3	6
	2nd roll	4.25	5.5	9.75	2.5	8
	3rd roll	5.25	5.75	11	2.5	7.7
C57BL/6 no. 2 (20.4 g)	1st roll	5	4.25	9.25	3.3	6.7
	2nd roll	5.25	6.75	12	2.5	8.4
	3rd roll	5.75	6.75	12.5	2.5	8.4
C57BL/6 no. 3 (20.5 g)	1st roll	4.5	5.25	9.75	2.5	7.3
	2nd roll	6.75	7.5	14.25	2.5	10.1
	3rd roll	6.25	6.75	13	2.5	9.5
Nude no. 1 (26.9 g)	1st roll	6	7	13	2.5	9.3
	2nd roll	4.75	5.25	10	2.5	7
	3rd roll	5.25	6	11.25	2.5	7.7
Nude no. 2 (24.2 g)	1st roll	3.5	2	5.5	2.5	4
	2nd roll	3	2	5	2.5	3.8
	3rd roll	3.25	2	5.25	2.5	3.9

Notes. The targeted maximum rotational speed of <3 revolutions/s (Hz) was achieved for 13/15 rolls for an average of 2.61 Hz. The average number of total revolutions was 10 for an average duration of 7.18 s. CCW = counterclockwise; CW = clockwise.